

Supplemental Material

Transcript Degradation and Noise of Small RNA-Controlled Genes in a Switch Activated Network in *Escherichia coli*

Rinat Arbel-Goren,¹ Asaf Tal,¹ Bibudha Parasar,¹ Alvah Dym,¹ Nina Costantino,²
Javier Muñoz-García,^{1,3} Donald L. Court^{2†} and Joel Stavans^{1†}

¹Department of Physics of Complex Systems, Weizmann Institute of Science
Rehovot 76100, Israel.

²Gene Regulation and Chromosome Biology Laboratory, National Cancer Institute
Frederick, MD 21702-1201, USA.

³Departamento de Matemáticas and GISC, Universidad Carlos III de Madrid
Av. de la Universidad 30, 28911 Leganés, Madrid, Spain.

Supplemental Table of contents

- Figure S1 Discrete nature of the intensity of spatially separable fluorescence spots.
- Figure S2 Effects of different mutant strains on the stoichiometric degradation of *sodB* and *fumA* transcripts with iron deprivation.
- Figure S3 Switch-like effects of iron deprivation on mean *sodB* levels obtained from qRT-PCR experiments.
- Figure S4 Effects of iron addition to an iron-free medium on the promoter activity of RyhB and one of its targets.
- Figure S5 Switch-like behavior of mean *sufC* transcript levels as function of iron deprivation.
- Figure S6 Effects of iron deprivation on target transcripts with which it does not undergo stoichiometric degradation.
- Figure S7 Ratios of promoter activities of RyhB and those of *sodB* or *fumA*, as a function of the concentration of DTPA.
- Figure S8 Graded monotonic production of YFP induced from an arabinose promoter.
- Figure S9 Effects of arabinose-induced RyhB production on the mean *sodB* transcript number.
- Figure S10. Effects of arabinose-induced RyhB production versus iron deprivation on *sodB* transcript noise.
- Figure S11 Effect of an RNase E mutant strain in which co-degradation is blocked on RyhB production.
- Figure S12 Average histograms of RyhB fluorescence density for three DTPA concentrations.
- Figure S13 Half-life of *sodB* transcripts for two DTPA concentrations obtained from qRT-PCR experiments.
- Figure S14 Effects of iron deprivation on cell growth.
- Table S1 Strains used in the study.
- Table S2 Sequences of smFISH probes, primers and probes used for qRT-PCR.

Supplemental Materials and Methods

Supplemental References

Supplemental Figures

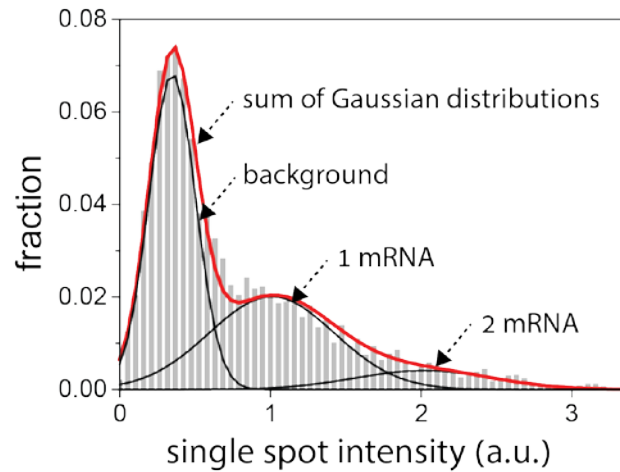


Figure S1 Discrete nature of the intensity of spatially separable fluorescence spots. Histogram of spot fluorescence intensity levels in smFISH images of *sodB* transcripts, at 0 μM DTPA. The histogram has been decomposed into a sum (red curve) of Gaussian contributions (black lines), each corresponding to a different discrete number of transcripts. The position of the peak corresponding to 1 mRNA was determined from a histogram obtained at 75 μM DTPA.

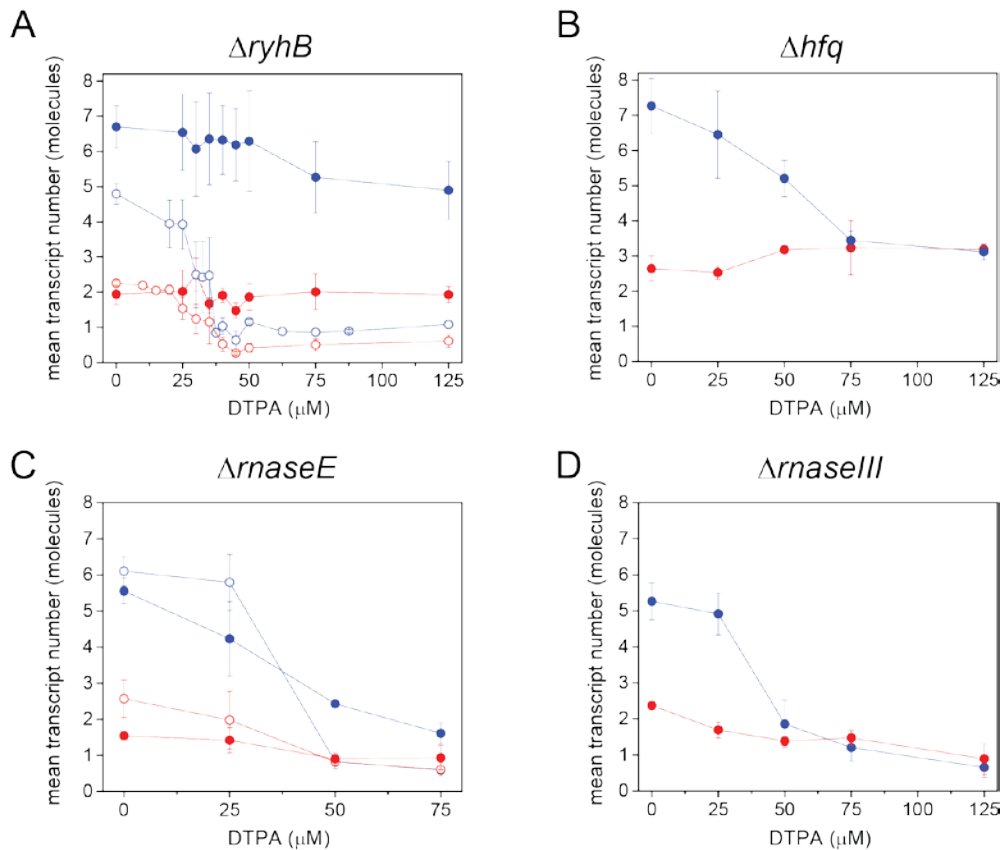


Figure S2 Effects of different mutant strains on the stoichiometric degradation of *sodB* and *fumA* transcripts with iron deprivation. Mean transcript numbers of *sodB* (blue) and *fumA* (red) in individual cells as function of the concentration of DTPA measured by smFISH, following procedures as described in Materials and Methods. (A) Measurements in a ΔryhB mutant strain (IRE-106). The transcript numbers are nearly independent of iron deprivation. For the sake of comparison, the corresponding data measured in the wild type strain (shown in Figure 2) is also plotted (empty circles). (B) Measurements in a Δhfq mutant strain (HL1188). The growth is severely affected in this strain. (C) Measurements in an RNase E mutant strain (TM528, *rne701-Flag-cat*, full circles) and in the background strain (TM338, *rne-Flag-cat*, empty circles). Activity in the RNase E mutant strain is not fully abrogated under iron deprivation. (D) Measurements in an RNase III mutant strain (NC499), show behavior similar to the wild type strain. The gradual reduction observed in the mean transcript number of *sodB* in all panels is due in part to a known reduction in the promoter activity of *sodB* with iron deprivation (1). Error bars denote standard errors over three independent experimental repeats.

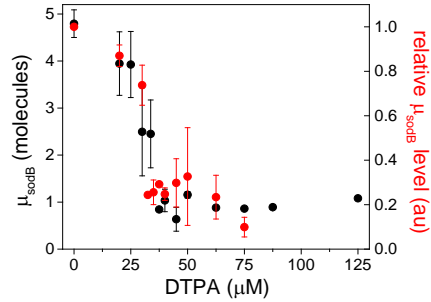


Figure S3 Switch-like effects of iron deprivation on mean sodB levels obtained from qRT-PCR experiments. Transcript sodB levels as a function of DTPA, normalized by the value without DTPA (red circles). Error bars denote standard errors from two independent experimental runs. Switch-like behavior is observed at $\sim 30 \mu\text{M}$ DTPA, in agreement with the data obtained from the smFISH experiments of Figure 2A shown for comparison (black circles). Cells were grown in the presence of different concentrations of DTPA and the sodB transcript level was measured using qRT-PCR techniques as outlined in Materials and Methods.

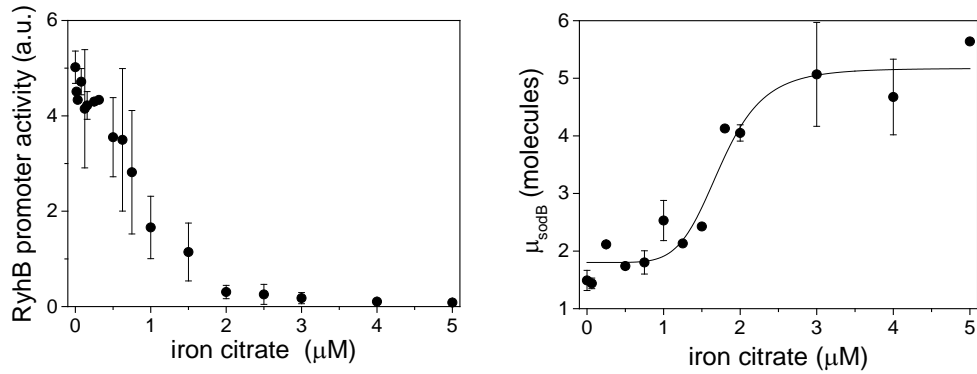


Figure S4 Effects of iron addition to an iron-free medium on the promoter activity of RyhB and one of its targets. *E. coli* cell cultures (MG1655 strain) were grown overnight at 37°C in LB medium, then diluted 1:50 into fresh M9 medium containing L-glucose (0.4%) and casamino acids (0.2%) and allowed to reach an OD₆₀₀ of 0.3-0.4. Cells were then further diluted 1:50 in the same medium, containing various ferric citrate concentrations and allowed to reach an OD₆₀₀ of 0.4-0.6. Left: Promoter activity of RyhB measured with reporter plasmids encoding a *pryhB-yfp* fusion. Right: Mean μ_{sodB} transcript number in individual cells as function of the concentration of iron citrate. Data were obtained from two independent experimental runs. Error bars represent standard errors. The black line through the data, represents a fit with a Hill function ($y = a + (b - a)(x^n / (k^n + x^n))$) with $a = 1.8 \pm 0.2$, $b = 5.2 \pm 0.4$, $k = 1.8 \pm 0.1$, $n = 6 \pm 2$. The value of the Hill coefficient 6 ± 2 in the present plot, albeit smaller than when adding DTPA to LB, is consistent with a high degree of cooperativity.

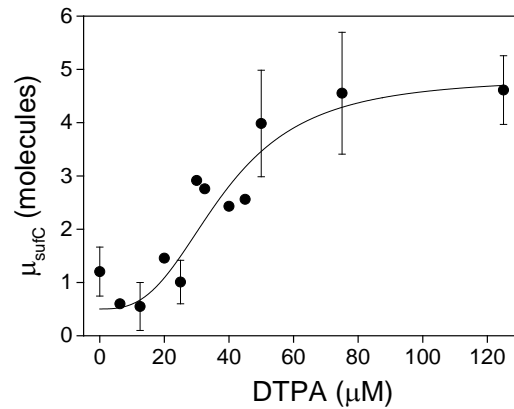


Figure S5 Switch-like behavior of mean *sufC* transcript levels as function of iron deprivation. Mean *sufC* transcript levels as a function of DTPA concentration, measured using smFISH. Note that *sufC* is under direct transcriptional repression by Fur but its transcripts are not RyhB targets. The data represent an average over three experimental runs carried out under the same conditions, while error bars denote standard errors. The black line through the data is a fit with a Hill function ($y = a + (b - a)(x^n / (k^n + x^n))$) with $a = 0.5 \pm 0.3$, $b = 5 \pm 1$, $k = 38 \pm 9$, and a Hill coefficient $n = 3 \pm 1$.

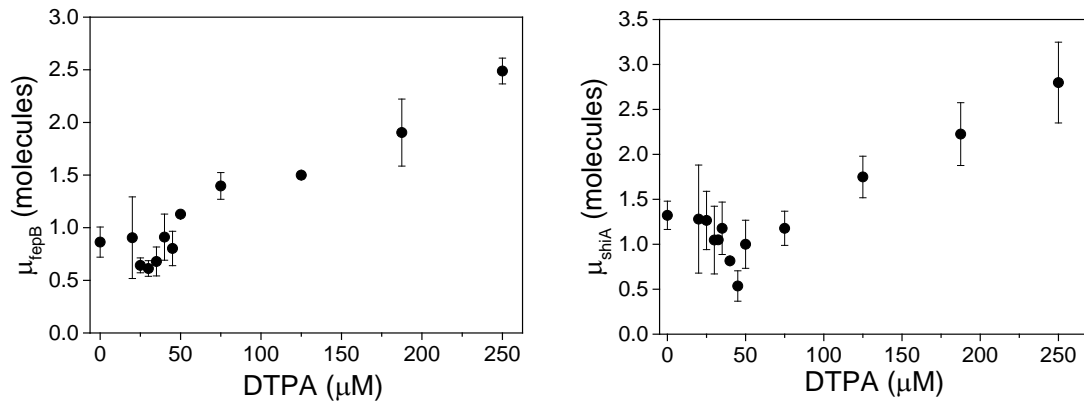


Figure S6 Effects of iron deprivation on target transcripts with which it does not undergo stoichiometric degradation. Left: mean fepB transcript number in individual cells as function of the concentration of DTPA. Binding of RyhB to fepB transcripts blocks the latter's Shine Dalgarno sequence, thereby inhibiting translation. Data were obtained from four independent experiments. Right: mean shiA transcript number in individual cells as function of the concentration of DTPA. Binding of RyhB to shiA transcripts activates translation by altering transcript secondary structure, exposing their Shine Dalgarno sequence. Data were obtained from four independent experimental runs. Error bars in both panels represent standard errors.

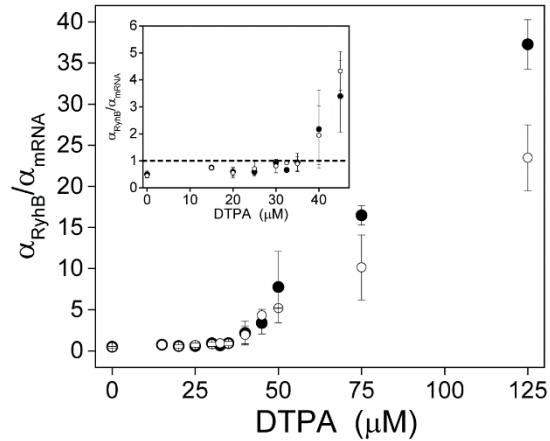


Figure S7 Ratios of promoter activities of RyhB and those of *sodB* or *fumA*, as a function of the concentration of DTPA. *E. coli* cell cultures (MG1655 strain) bearing plasmids with the promoter fusions of either *ryhB*, *sodB* or *fumA* to YFP were grown overnight at 37°C in LB medium, then diluted 1:50 into fresh LB medium and allowed to reach an OD₆₀₀ of 0.3-0.4. Cells were then further diluted 1:50 in the same medium for 3 hours. The values of the promoter activities of the three genes α_{RyhB} , and $\alpha_m = \alpha_{sodB}$ or α_{fumA} were measured simultaneously in a plate reader as a function of DTPA concentration (see Materials and Methods). Shown are the ratios α_{RyhB}/α_m of either *sodB* (empty circles) or *fumA* (full circles). Data were obtained from two independent experimental runs. Error bars represent standard errors. Inset: blowup of the small DTPA portion of the data, illustrating that the value at which the rate of production of RyhB is equal to the rates of production of *sodB* and *fumA* is accessible in our experiments (dashed line).

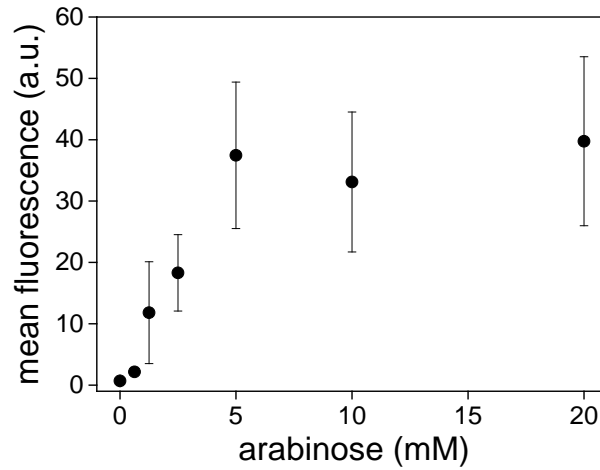


Figure S8 Graded monotonic production of YFP induced from an arabinose promoter. *E. coli* cell cultures (strain IRE-111) were grown overnight at 37°C in LB medium, then diluted 1:100 into fresh LB and allowed to reach an OD₆₀₀ of 0.3-0.4. Cells were then further diluted 1:40 in LB containing various arabinose concentrations for 3 hours and then diluted 1:5 in M9 medium with the same arabinose concentration in a 96-well plate. Plates were maintained at 37°C with shaking throughout the YFP fluorescence and optical density (OD₆₀₀) measurements. The mean fluorescence was obtained over six independent replicates and the error bars represent standard deviations.

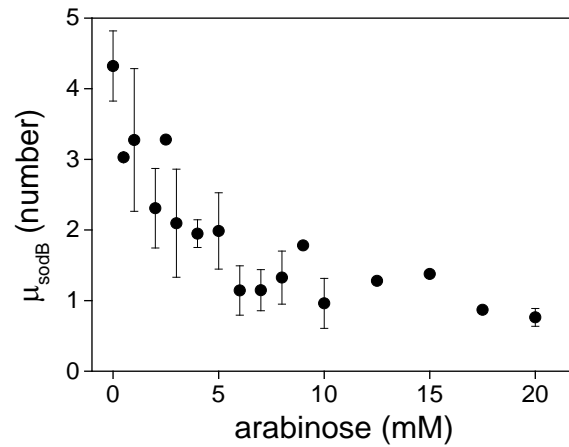


Figure S9 Effects of arabinose-induced RyhB production on the mean *sodB* transcript number. Mean *sodB* transcript number in individual cells as function of the concentration of arabinose measured using smFISH in a strain in which RyhB is produced from an arabinose-induced promoter (IRE-109). The fluorescence represents the mean over three independent experiments and the error bars represent the standard error.

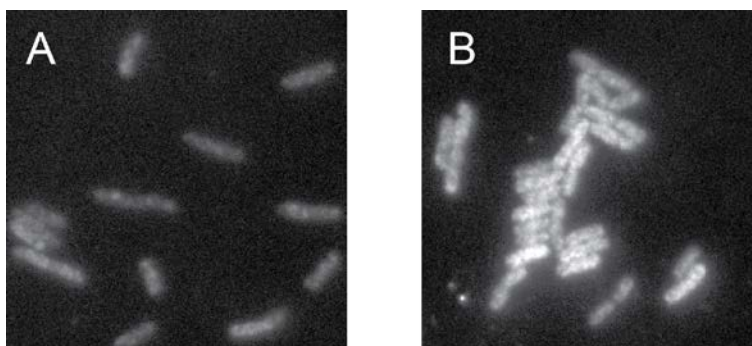


Figure S11 Effect of an RNase E mutant strain in which co-degradation is blocked on RyhB production. Typical snapshots of fluorescence from undegraded intracellular RyhB, tiled with labeled oligonucleotides. Panel A: background strain (TM338). Panel B: in an RNase E mutant strain (TM528). Both images were taken at iron-poor conditions (75 μ M DTPA).

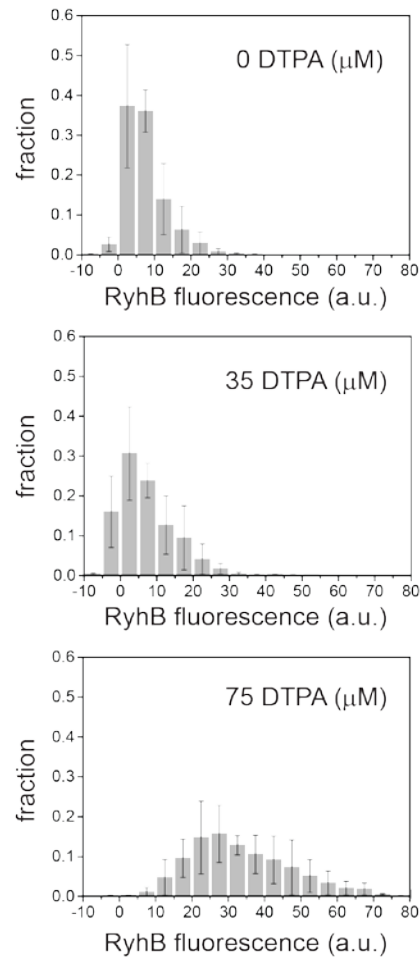


Figure S12 Average histograms of RyhB fluorescence density for three DTPA concentrations. Fluorescence density is defined as fluorescence measured in individual cells, normalized by their area. Cells were grown, treated with DTPA and RyhB was labeled as described in Materials and Methods (main text). The average histograms correspond to RyhB distributions measured at DTPA concentrations below (top), above (bottom) and within the switching region (middle) (see Figure 4B). The average histograms represent bin-by-bin means of histograms measured in three independent experimental runs, while errors bars represent standard errors. Prior to calculating histograms within each run, the average background fluorescence measured in a $\Delta ryhB$ strain was subtracted from the fluorescence in the wild-type strain.

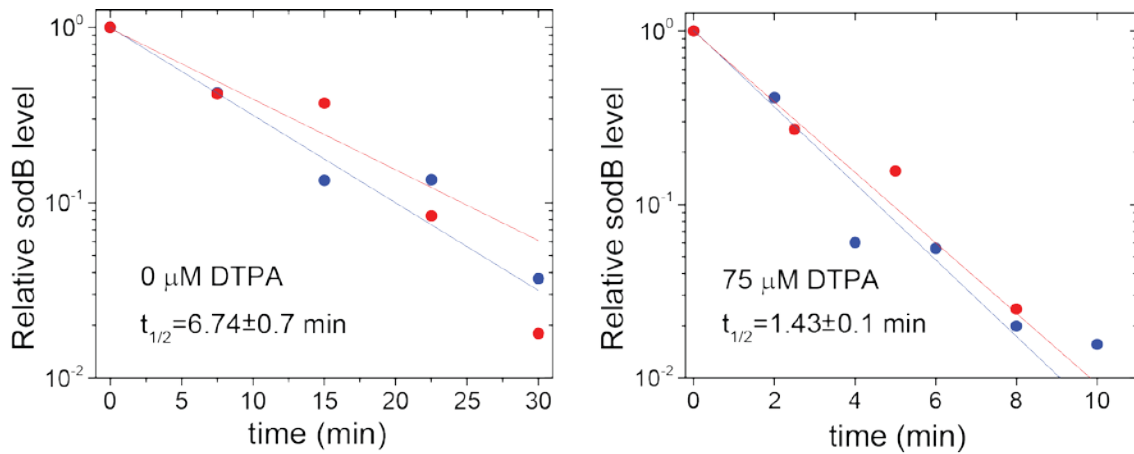


Figure S13 Half-life of *sodB* transcripts for two DTPA concentrations obtained from qRT-PCR experiments. Relative level of *sodB* transcripts as a function of time after addition of rifampicin, measured using qRT-PCR for $0 \mu\text{M}$ and $75 \mu\text{M}$ DTPA. Two independent repeats were performed in each case (red and blue circles). The corresponding red and blue lines represent linear fits to the data, the inverse of the slopes yielding the corresponding half-life. The shown values of the half-life $t_{1/2}$ represent an average over the corresponding two experiments in the plot while errors represent standard errors.

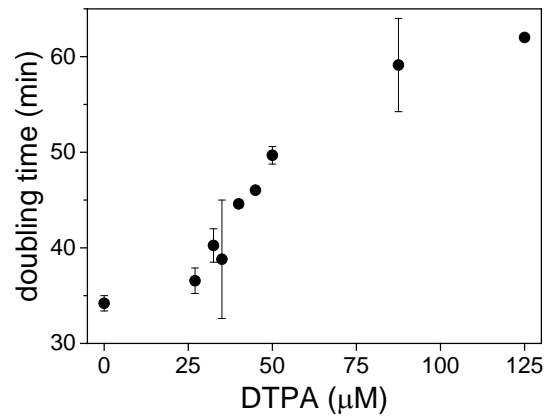


Figure S14 Effects of iron deprivation on cell growth. Mean doubling time of cells as function of DTPA concentration. *E. coli* cell cultures (MG1655 strain) were grown overnight at 37°C in LB medium, then diluted 1:100 into fresh LB and allowed to reach an OD₆₀₀ of 0.3-0.4. Cells were then further diluted 1:80 in LB containing various DTPA concentrations under the same growth conditions at 37°C as in the smFISH experiments and after 2.5 hours the optical density (OD₆₀₀) was measured as a function of time in a 96-well plate. Plates were maintained at 37°C with shaking throughout the experiments. The data represent an average over two experimental runs carried out under the same conditions. Error bars denote standard errors. Each experiment was repeated at least twice on different days.

Supplemental Tables

Table S1 Strains used in the study

Strain Name	Strain #	Mutations	Reference
WT-Keio	BW25113		(2)
Δ sodB	JW1648	<i>sodB734(del)::kan</i>	(2)
Δ fumA	JW1604	<i>fumA760(del)::kan</i>	(2)
Δ sufS	JW1670	<i>sufS757(del)::kan</i>	(2)
Δ shiA	JW1962	<i>shia755(del)::kan</i>	(2)
Δ fepB	JW0584	<i>fepB730(del)::kan</i>	(2)
WT	MG1655		(3)
Δ ryhB	EM1238	<i>ryhB::cat</i>	(4)
Δ ryhB	IRE-106	Δ araFGH Δ araE <i>ryhB<>cat</i>	New strain
P_{BAD} - <i>ryhB</i>	IRE-109	Δ araFGH Δ araE <i>ryhB<>cat</i> P_{BAD} - <i>ryhB</i>	New strain
P_{BAD} - <i>yfp</i>	IRE-111	Δ araFGH Δ araE <i>ryhB<>cat</i> P_{BAD} - <i>yfp</i>	New strain
<i>rne-Flag-cat</i>	TM338	<i>rne-Flag-cat</i> ,	(5)
<i>rne701-Flag-cat</i>	TM528	<i>rne701-Flag-cat</i>	(5)
<i>rnc14</i>	NC499	<i>rnc14::miniTn10</i>	New strain
Δ hfq	HL1188	<i>hfq::cat</i>	New strain

Table S2 Sequences of smFISH probes

Gene	<i>ryhB</i>	<i>sodB</i>	<i>sufC</i>
Probe	Stellaris® FISH Probes, Custom Assay with CAL Fluor® Red 590 Dye	Stellaris® FISH Probes, Custom Assay with CAL Fluor® Red 590 Dye Or Stellaris® FISH Probes, Custom Assay with Quasar® 670 Dye	Stellaris® FISH Probes, Custom Assay with CAL Fluor® Red 590 Dye
Probe sequences (5' to 3')	CTTTCAGGTTCTCCGCGAGG AAGCAATGTGAGCAATGTCG CCGGCTGGCTAAGTAATACT	GTGCAGGTAATTCGAATGAC AGAGCATCTTTAGCATATGG TTCCGCAGAAATGTGCGGTG TGCCGTAGTGATACTCGATG GTGACATAAGTCTGATGGTG CGGTACCTTTAATCAGGTTG TTCCAGTGATTTACCTTCAA CCTTCAGAGCTGCGAATAAT CTGAGCTGCGTTGTTGAATA GGCAGTTCAGTAGAAAAGTA TTCAGCGACTTTTCCAGTCG TGCCAAAAGATGCGGCGATA TGCGCTTTGAAATCGGCAAA TTTGATCGCTGCATCAGTAA AGGTCCAGCCAGAACCAAAG TTTGCCATCGCTGTTTTTCA CCGCGTTAGAGGTTGAAACG ATCAACGGTCAGCAGCGGAG ATGTAATAAGCGTGTTCCTA AGGACGTGCATTGCGATAGT CCCAGAAGTGCTCCAGATAG CGGAGATTTTTTCGCTACGAA	CGCTGACGTGTAATCTTTA CGCAGGATAGCTTTATCTTC GGATGAACGTCGAGGCTTAA CCATAATGGCGTGAACCTCG GTTGCCGATAAGGTACTTTT CACTTCATAATCTTCTCGCC CTTTGAACTCAACCGTGCCG CGACAGCGCAAGCAAATCTT AAGGCCATAAAGATGCCTTC TGGTTACTGACACCTGGAAT TAAGTGCCGTTTGCAGGAAA AAATCAAAGCGGTCGAGCGT TTTCTCTCCATCAAATCCT AAATCTCCGGCATCTTCAG AACGTTTACCGAACGGGTTA TTTTCTCGCCGCCGAAAAA CCGCCATTTGCAAAATATCG TCCGACTCATCAAGAAATGCA ATCGGCGACCACTTTTAATG CATCACGCAGCGAGTTCACG ACAATGATGAATGAGCGCTT GAGAATGCGTTGGTAGTGCG CGTAATCAGGCTTGATGTAG CGTCCCTGATATAGCACATG GAAATCGCCGGATTTACAAA CCTCCAGTTGTTTGACCAAC TTCGGTAAGCCAGCCATAAC

Gene	<i>fumA</i>	<i>fepB</i>	<i>shiA</i>
Probe	Stellaris® FISH Probes, Custom Assay with CAL Fluor® Red 590 Dye	Stellaris® FISH Probes, Custom Assay with CAL Fluor® Red 590 Dye	Stellaris® FISH Probes, Custom Assay with CAL Fluor® Red 590 Dye
Probe sequences (5' to 3')	GCTGGTTAGCAGGTAATACT ATTACAGATACGCTAACGTGT GCGACTTTCAAATCTCCTG CAACAGAGTTAACGCTTCGG ATGAACGACGCATCATGAAA TTTATCATTTTCGCTGGCCT GAGTTACGCAGGAATTGCAG GTATCCTGACAGGTTGGCAG TACCAACAATAATCGCGGTG TAAGTGTATATAGACACCGCG AGTAGCGCAGATTATCTTTCG TTTATACATATCCAGCGGCG CAGATTGGTGCCGGTATTCA CATAAAGATCGATCTGCGCT TTTGTATTTCGTCGCCATCAA CCACCTTTGGCGATACAGAG GATACGTCTTGTTCGCCGAA AACGCTTTGGTTTCCTGATA GCATCTTCTCAACCAGGTAA ATATGATACGGAGGACAGGC AGTTCCACCAATAACGAACG CCGTTTTAAGGTTTCGTTTCT TATTTTCGCGAAGCCAGTTT TTCCGTTGGCAGTTCATCAT TTTTCCAGTTCACATCGCG AAGATTTTTCGCTTCGATCA CGTGAGCGAAGTATTTACCA TATTACGGTCAGCAGAGCAG TGACGGTTGATCTTCGCTTT TGTTCCAGTTTTTCGATCCA TTCCGGGATATATTTGCCTG ATCGGACGGTTAAGGTCAAC CAACTGTGCGAGGATCTCTT GTGTAGAAACGGGATACTGC ATAATCGTGCCGTTAAGCGA GTGAGCAATATCACGACCGA CCATCCGCTCTTTCAGTTTTG	CCTGTTAATAGAAGGGCGTT AACTGCGGCTATTCCTGAAA ACGGCTGTCAGTAATCTGAC CTGGCTTTCCAGTGTATGTG CGCTGGTGAAACAATACGC GATCACCGGAGCATCAATCG TTGCTCCACTGGCGTAAAAA TTGCAGTTTTCGCTTCTTTCG CTCGGTTTCGCCGATATAGAG GCCGTTGCGCTAATTAATA AAAGCTGATCATAACAGTGCC TGATTAATGTCCGGGCGATG CAGCTTTTGTTCGTCGTAATT AAGTTGCGTTAACAGCGACT TTTCTCATGCCCGGTAATTT AGTTGCTTATCAAATGCGC GCGGTAATTTGATTTGCTCT ATAGACAATGGCAGTGACCG ATTCTGGCGTCCAGAGATTG AGCGTAAAGCCGAGTTGTTT CATTTAACCTGCGGGTAAAC TGCGGTTTACCCTGACTTTG CCCACCAAGCTGAATGATGT ATTTAACCTGACGCCAGAT GGCGAACAGGAATAGTGACT CATCGGCATCTTTCTGATCA CGAGCAGCGGATTAGCATAA CGCATAAACCTGCTTGTTTT CAGACGGAACGTCTCGGTTT CTTGATGGCGCTGTAGTAA AAAAACAGCGCCTTAAGCCTA	ATCGGGACGAGTGGAGATGA CGGGCGGACTTAACGAAAG ATCATACCAGTCGACGACGG CGGTGATGCCATAGAGTAAA TCGCGATTAAACACCACTGC CGGGCTTACTTGCGGGAAAA ACGCCAAAGGTAGCAATGC GCCGAGCGGACGGAAAAAGAA GTCGCCAAAGTGACCGAAAA TCAGCATTAACATGCGCTTA CAATCAAGGCTGTGCGGATG CACCCAATGGTCGAGAATGA GCAGTGTCAACGACGAAATA CGACTGCAAAATCCCTGAATG TTCAACGGAAAGCAACGCCG GCTTTTTTATTTTTTCGGTGC CTTGTACACCGCTACTGTAA CAGTAAACCTACACCGTAGC AATGAAACCGATCCGGTTGA GTCAGTCGTATCATATACTGA CAGCCCCAGCTTAAAAACTG CAGTACCAGTACGATGCTAA TTGTTCAAATCCGCGGACT CGGCAGCTTGATAATGTTGC ATAACCGGGATGCGTTTTTTT AAAGCAACCGGATGTCGTAA TCGTAGCGCAATAATCTTCA ACATCGTCAGCAATTCGCAC AGTGCAAAGGCAGTAACGAT CCCATATCTGGGTTGAATA AAGGAAAAGTTCGCGCGGTA CACCTACCAGCAAACCAATA GGAATTGTGAGGCAGCTTAA ATCGGCAAGCCAGGCAAAAC AAACCTACGGCGACCAAAA CCGATTAACGTACCTGTGAT GAAAGGAAATGCGCTCAACG ATAGATTGTGCTTCAAGCGC TGCCAGCATTATGGAGAAGA ATCGGTTGTTGCACACACAC GGCACCAAAACATTTTCGGTAA CAGCGCCACTATAGCGATAA CACACTGGCAACCTGATAAC GCAGCGGCAATAAAAGGTGT TCCCGGCAAAGTAAGTGATG GCATCCAGCCAGCAAAATAA AAGCGGTCATTGCGGAAATC CGTTGACTGTCTTTCATCAA

Primers and probes used for qRT-PCR

Oligo name	Sequence
<i>sodB</i> F' primer	ACC GCG TTT GAA GGT AAA TCA
<i>sodB</i> R' primer	GAC CTG AGC TGC GTT GTT GA
<i>rpsL</i> F' primer	AAG CGT CCG TTC TAC CAG GTT
<i>rpsL</i> R' primer	AAC CAA CGC GCT CGA TGA
<i>sodB</i> probe	6-FAM-TTA TTC GCA GCT CTG AAG G-MGB
<i>rpsL</i> probe	6-FAM-TTG TCG CTG ACA GCC G-TAMRA

Supplemental Materials and Methods

Expression of the arabinose *pBAD* operon following induction with limiting levels of arabinose results in some cells being fully induced and others remaining un-induced for *araBAD* operon transcription. Induction by arabinose is autocatalytic and the first cells to take up some arabinose are induced to express transport functions AraFGH and AraE allowing the uptake of more arabinose (6). This all-or-nothing induction of the *pBAD* promoter is prevented by using a strain deficient in both *araE araFGH* as well as the catabolic functions (*araBAD*). Morgan-Kiss *et al.* demonstrated that in such an *ara* mutant strain, a particular LacY protein mutant could perform facilitated diffusion of arabinose resulting in homogeneous and graded expression of the *ara* promoter over extended incubation times at sub-saturating levels of arabinose (7).

Deletion of the arabinose transport genes *araFGH* and *araE*. The *araFGH* cluster was deleted by a two-step selection/counter-selection process using recombineering methods (8). We started with strain IRE101, which is MG1655 with the pSIM18 hygromycin resistant plasmid used to express the Red recombineering functions (9). First, the *tetA-sacB* cassette was inserted by recombineering methods into IRE101 to replace *araFGH* using selection for tetracycline resistance conferred by the *tetA* gene and sensitivity to growth on LB sucrose conferred by the *sacB* gene, thereby generating the strain IRE102. Next, recombination with oligo RY17 and selection for sucrose resistance, created the clean deletion of the *araFGH* cluster from IRE102 and removal of the *tetA-sacB* cassette. RY17 contains the sequence 5'GTG GGA AAA AAC GCT AAA TTG TTG CAG AAA AAA GCA / TTG TCT TTG GTA CCC ATG CGG GAT GTC TTC TTT TTA 3' where the / defines the deletion endpoints to each side of the *araFGH* segment in the new strain IRE103.

The *araE* gene was deleted from IRE103 in a similar two-step selection/counter-selection process using recombineering methods (8). First, the *tetA-sacB* cassette was inserted to replace *araE* using selection for tetracycline resistance conferred by the *tetA* gene. Recombinants were tested for sensitivity to growth on sucrose conferred by the *sacB* gene, thereby generating the strain IRE104. Next, recombination with oligo RY12 and selection for sucrose resistance, created a clean deletion of the *araE* gene from IRE103 and removal of the *tetA-sacB* cassette. RY12 contains the sequence 5'AAT GTT CAG CGC AGT GTA GAG CCA GAA CGT ACC GGC / TTC AAA TTA AGT TGA ATT ATT GAG ATT ATT AAC 3' where the / defines the deletion endpoints to each side of the *araE* gene in the new strain IRE105.

Deletion of the *ryhB* gene to generate strain IRE106. In the strain IRE105 (MG1655 Δ *araFGH* Δ *araE* /pSIM18), the native *ryhB* gene was replaced with a *cat* cassette (*ryhB*<>*cat*) conferring chloramphenicol resistance by the process of recombineering. The *cat* cassette was amplified by PCR with primers carrying 50 nucleotide long regions at their 5' ends homologous to each flank of the *ryhB* gene. RY18 and RY19 are the two oligo primers used to generate the *cat* cassette with 50bp flanking homologies. RY18: 5' TTT

GCA AAA AGT GTT GGA CAA GTG CGA ATG AGA ATG ATT ATT ATT GTC TCT GTG ACG GAA GAT CAC TTC G and RY19: 5' TAA CGA ACA CAA GCA CTC CCG TGG ATA AAT TGA GAA CGA AAG ATC AAA AAA CCA GCA ATA GAC ATA AGC G where each underlined sequence is the primer segment for *cat* cassette amplification. The region upstream of RY18 and RY19 is the homologous segment upstream and downstream respectively of the *rhyB* gene.

Insertion of *ryhB* under *araBAD* promoter control. Starting with the strain IRE106 (MG1655 Δ *araFGH* Δ *araE* *ryhB*<>*cat* strain carrying pSIM18), we inserted the *ryhB* gene under transcriptional control of the *araBAD* promoter in a precise way so that the native *ryhB* 5' RNA end is in the position of the native *pBAD* 5' RNA start and at the same time removed the entire *pBAD* RNA coding region for the *BAD* genes and replacement with the *rhyB* gene. First, phage P1 was grown on the strain XTL298 that carries the *tetA-sacB* cassette in place of the *araBAD* genes with the *amp* gene also present just beyond *sacB* as described previously (8). This cassette was transduced by P1 into IRE106 so as to generate IRE107 (MG1655 Δ *araFGH* Δ *araE* *ryhB*<>*cat* *araBAD*<>*tetA-sacB amp*). Next the *ryhB* gene was amplified to encode from the first nucleotide of *RyhB* RNA through the 3' end of the RNA by PCR using primers carrying 50 nucleotide long regions at their 5' ends. One homologous to the regions just upstream of the *ara* RNA start and the second homologous to the DNA beyond the *tetA-sacB amp* cassette. RY21 and RY20 are the two oligo primers used to amplify *ryhB* with their respective flanking homologies. RY21: 5' AGC GGA TCC TAC CTG ACG CTT TTT ATC GCA ACT CTC TAC TGT TTC TCC ATG CGA TCA GGA AGA CCC TCG C and RY20: 5' GCT TGA GTA TAG CCT GGT TTC GTT TGA TTG GCT GTG GTT TTA TAC AGT CAG ATT TCG TCC TTT TTA AGG TGG TTA TTT ACA C where the underlined sequence corresponds to sequences priming amplification of the *ryhB* gene. This *ryhB* DNA cassette with flanking homologies was used to replace the *tetA-sacB* counterselection cassette and fuse *RyhB* expression to the *pBAD* promoter by recombineering and selection of sucrose resistant recombinants. The final strain IRE108 is MG1655 Δ *araFGH* Δ *araE* *ryhB*<>*cat* *P_{BAD}* – *ryhB* in which the pSIM18 plasmid (whose replication is temperature sensitive) has been eliminated by continued growth at 42 degrees (9).

LacY permease mutant expressed from the plasmid *placYA177C.** Plasmid *placY**A177C constitutively expresses a permease capable of facilitating diffusion of arabinose into cells at sub-saturating levels (5). This plasmid was transformed into the IRE108 strain (MG1655 Δ *araFGH* Δ *araE* *ryhB*<>*cat* *P_{BAD}* – *ryhB*) to generate strain IRE109.

Insertion of *yfp* coding segment under the control of the *araBAD* promoter and the translation initiation codon of *araB*. The strain IRE110 was made and used to generate a strain with *yfp* under control of *pBAD*. Strain IRE105 (MG1655 Δ *araFGH* Δ *araE* /pSIM18) was transduced by P1 to insert *araBAD*<>*tetA-sacB amp* to be used for counterselection and replacement with *yfp*. The *yfp* gene was amplified from its ATG start codon through the stop codon using primer RY28 and RY29 that carry 50 nucleotide long regions at the primers 5' ends. RY28 has homology to the region just upstream of the *araB* start codon, and RY29 has homology to the DNA beyond the *tetA-sacB amp* cassette. Recombination with these PCR products deletes the *araBAD* operon and precisely replaces all their open

reading frames with the open reading frames of *yfp* beginning at the ATG of *araB*. Note that *yfp* and *cfp* are identical in sequence at the 5' and 3' ends of their coding sequences, and thus the same primers can be used for both genes. The Yfp expressing strain is IRE111 and is MG1655 $\Delta araFGH \Delta araE ryhB \langle \rightarrow cat P_{BAD} - yfp$. RY28: 5' ACT CTC TAC TGT TTC TCC ATA CCC GTT TTT TTG GAT AGG AGG ATG AAA CGA TGC GTA AAG GAG AAG AAC TTT TC, and RY29: 5' GCT TGA GTA TAG CCT GGT TTC GTT TGA TTG GCT GTG GTT TTA TAC AGT CAT TAT TTG TAT AGT TCA TCC ATG CC where the underlined sequence corresponds to sequences priming amplification of the *yfp* gene. The pSIM18 plasmid whose replication is temperature sensitive was eliminated from both by continued growth at 42 degrees (9). The Ampicillin resistant plasmid *placY**A177C, which constitutively expresses the LacY permease capable of facilitating diffusion of arabinose into cells at sub-saturating extracellular levels (7), was transformed into and is present in final IRE113 and IRE114 strains.

RNAase III mutant *rnc14* in MG1655.

An RNAase III mutant containing a mini-Tn10 insertion in the *rnc* gene (*rnc14*) has been described (10). The *rnc14* mutation was moved by P1 transduction (12) to MG1655 and designated NC499. NC499 has the same phenotype as other *rnc* mutants (10).

Hfq deletion mutant in MG1655.

HL1188, from the Gottesman lab (S. Gottesman and H. Li) was made by moving *hfq::cat* into MG1655 by P1 transduction, and selecting for CmR from a strain TX3077 referenced in <http://www.ncbi.nlm.nih.gov/pubmed/9393714>.

Recombineering: Recombineering methods and protocols performed are described (see: <http://redrecombineering.ncifcrf.gov/>) (11, 13). In strain construction of gene replacements by drug markers, there was a two-hour outgrowth, and then the cells were plated on appropriate antibiotic plates (30 μ g/ml ampicillin, 10 μ g/ml chloramphenicol, 12.5 μ g/ml tetracycline, 50 μ g/ml kanamycin).

Sequencing and Analysis: Final gene constructions made by recombineering protocols were sequenced. Sequencing was done by Leidos Biomedical Research, Inc. Sequencing results were analyzed with Sequencher version 4.8.

Oligos and bacterial strains : Gene replacements were made by dsDNA recombineering (13); construction details including final construct sequence will be supplied upon request. Multiple mutants were introduced by P1 transduction (14). Oligos were purchased from Integrated DNA Technologies (IDT) and were desalted but not further purified.

Single-molecule fluorescence *in situ* hybridization (smFISH): We followed already published procedures (15).

Probe design and labeling: DNA oligonucleotide probes were designed using the Stellaris RNA probe FISH designer (<https://secure.biosearchtech.com/stellarisdesigner/>). The Stellaris™ FISH probes were tagged with CAL Fluor® Red 590 dye or with Quasar® 670 dye. Sequences of smFISH probes are given in the Supplementary Table S2. The probes were dissolved in 10mM Tris-HCl 1mM EDTA (pH 8.0) to create a probe stock at a total oligo concentration of 25 µM. The tube was wrapped in aluminum foil and stored at -20 °C.

Sample fixation and permeabilization: Overnight cultures of the indicated *E coli* strain deletions from the KEIO collection (2) and an MG1655 *E coli* strain, were diluted 1:100 in 4 ml of LB medium. The culture was incubated at 37 °C with shaking. When OD₆₀₀ of the culture reached 0.3–0.4, the cells were pelleted by centrifugation (5 minutes, 4500×g, 4°C). The supernatant was removed and the cells were resuspended in 1 ml 1× PBS (Diethylpyrocarbonate (DEPC)-treated) and 4 ml freshly prepared 4.6% formaldehyde. The cells were then mixed on a rotator at room temperature for 30 minutes. The cells were pelleted by centrifugation (10 minutes, 1000×g, 4°C). The supernatant was removed and the cells were washed in 1 ml 1× PBS twice (i.e. re-suspended in 1 ml 1× PBS, centrifuged at 1000×g for 7 minutes, 4°C, and supernatant removed). The cells were re-suspended in 300 µl (DEPC)-treated water, and then 350 µl of 100% ethanol was added and mixed twice to get to a final concentration of 70% ethanol. The cells were left at room temperature with mixing on a rotator for at least 1 hour (or alternatively, at 4 °C for at least an overnight) to permeabilize the cell membrane.

Hybridization: After permeabilization, cells were centrifuged (7 minutes, 750×g) and the supernatant was removed. The cells were resuspended in 1 ml of 20% wash solution (0.2 g of formamide in 1 ml of 2×SSC (DEPC treated) and the tube was left standing for a few minutes. An aliquot of 20% hybridization solution (10 ml of 20% hybridization solution filter sterilized which contains 1 g of dextran sulfate, 2 g of formamide, 10 mg of *E. coli* tRNA, 1 ml of 20× SSC, 40 µl of 50 mg/ml BSA and 100 µl of 200 mM ribonucleoside vanadyl complex) was warmed to room temperature and 50 µl was added to a microcentrifuge tube. The indicated Fish probes were added at final concentration of 250 µM to the hybridization solution and mixed well. The cells were then centrifuged (7 minutes, 600×g) and the supernatant was removed. The cells were resuspended in the hybridization solution with probes and left at 30 °C overnight. Hybridized samples could be stored at 4 °C.

Washing: 10 µl of hybridized sample was transferred to a microcentrifuge tube. The rest was stored at 4 °C. 1ml of 20% wash solution was added to the tube and mixed well. Cells were pelleted by centrifugation (7 minutes, 750×g) and the supernatant was removed. The cells were washed 2 more times in 1ml of 20% wash solution, centrifuged at 750×g for 7 minutes, and supernatant removed). The cells were resuspended in 25 µl of 2× SSC and imaged under the microscope.

Transcript visualization : An agarose gel pad (1.5%) in SSCx2 was made on a coverslip and 5 μ l of sample was pipetted onto the pad and a #0 mm coverslip was placed on top of the agarose gel pad. The sample was imaged on a Nikon Eclipse –Ti-E microscope controlled by the Niss elements software using a 100x N.A 1.45 oil immersion phase contrast objective lens (Nikon plan-apochromat 100x 1.45 lambda) and an Andor iXon X3 EMCCD camera. All the filters are from Chroma. The filters used were ET-534/30x for excitation, 560lp as dichroic mirror and ET-585/40M for the emission. A phase contrast image was acquired followed by a z-stack of 13 slices and 250 nm spacing of fluorescent images with 2s integration time of each slice. Each sample was imaged at multiple locations to get a total of at least 500 cells.

Spot recognition: A spot recognition program developed in our lab, based on a version of the IDL ParticleTracking software (www.physics.emory.edu/~weeks/idl/) (16) adapted to Matlab by D. Blair and E. Dufresne (<http://physics.georgetown.edu/matlab>), and incorporated into our custom Matlab program (2), was used to automatically identify and quantify localized fluorescence signals. A Gaussian filter was first applied to smooth out noise, and spots were recognized by the presence of a local maximum in both x- and y-directions. This was done at each z-position in the stack of images, and each spot was quantified at the z-position where it had the highest fluorescence intensity (where the spot is in focus).

Estimating mRNA numbers: A fluorescence spot could consist of multiple mRNAs in close proximity. The integrated intensity arising from a single mRNA needed to be estimated for each smFISH experiment so that fluorescence intensities could be normalized to give the absolute number of mRNAs. The typical intensity of “false positives” in an experiment was first estimated from the histogram of individual spot intensities of a negative control (e.g.: *E. coli* strains Δ sodB or Δ ryhB). Histograms of individual spot intensities from relatively low expression samples (exposed to 125 μ M DTPA) were then examined. Because most spots in these samples were expected to contain a single mRNA, the first peak in the intensity histogram that emerged above the false positive range served as an estimate for the intensity of a single mRNA. The sum of intensities of all spots in each cell was then normalized by the single mRNA intensity to give the absolute number of mRNAs.

Quantitative reverse transcription polymerase chain reaction (qRT-PCR) RNA lifetime measurement: RNA lifetime measurements were carried out following the previously published methods (15). Cells were diluted from overnight cultures and grown in a 25 ml volume, under the same growth conditions with or without DTPA as in smFISH experiments. When OD₆₀₀ reached \sim 0.3, the culture was separated into two halves, each half being transferred to a new culture flask, and grown at the same conditions for 10-15 minutes. 1.5 ml of culture was then extracted from each flask and mixed with 3 ml of Qiagen RNeasy Protect Bacterial reagent to stabilize cellular RNA (see **Total RNA extraction** below for details). These samples were treated as $t = 0$ samples. Rifampicin was at $t=0$ added to one of the remaining cultures, at a final concentration of 500 μ g/ml, to inhibit

transcription. The culture without rifampicin served as a control. 1.5 ml of culture was extracted from each flask at 0, 7.5, 15, 22.5 and 30 min for 0 μ M DTPA and at 0, 2, 4, 8, 10 min for 75 μ M DTPA after addition of rifampicin and mixed with 3 ml of Qiagen RNeasy Protect Bacterial reagent to stabilize cellular RNA. Subsequent total RNA extraction and qRT-PCR were performed as described previously in this section. Target RNA level of the rifampicin-treated sample as a function of time was fitted to an exponential, $\ln y = Ax + B$ and RNA lifetime (in minutes) estimated as $\tau_{RNA} = -1/A$.

Total RNA extraction: Two volumes of RNeasy Protect Bacteria Reagent (Qiagen) were added to bacterial cell cultures that reached $OD_{600} = 0.3-0.4$. Total RNA was then extracted using the RNeasy Mini Kit with the optional DNase I digestion step (RNase-free DNase Set). The eluted from the final step was passed through the spin column one additional time to increase total RNA concentration. 2 μ l of each total RNA sample diluted 10-fold in 10 mM Tris-Cl, pH 7.5 was measured on a Nanodrop. The purity and concentration of the total RNA samples were estimated from the absorbance spectrum between 220 and 320 nm. The samples were treated with DNase I for 30 minutes at 30 $^{\circ}$ C (using a DNA-free: DNase treatment & removal kit).

Reverse transcription: The RNA was then reverse transcribed to get the corresponding cDNA. Reverse transcription was performed immediately after the total RNA extraction. The cDNA was synthesized using High Capacity cDNA Reverse transcription kit following the manufacturer's protocols. The optional RNase inhibitor was used in the reaction. The 2X RT master mix was prepared by mixing 2.0 μ l of 10X RT buffer, 0.8 μ l of 25 X dNTP mix (100 mM), 2.0 μ l of 10X random primers, 1.0 μ l of MultiScribeTM Reverse Transcriptase, 1.0 μ l of RNase Inhibitor and 3.2 μ l of RNAase-DNase free PCR water to make a final volume of 10 μ l total reaction. The thermal reaction was performed as follows: 25 $^{\circ}$ C for 10 minutes; 37 $^{\circ}$ C for 120 minutes; 85 $^{\circ}$ C for 5 minutes; 4 $^{\circ}$ C for storage. The cDNA samples were then diluted to a final concentration corresponding to a RNA amount of 20 ng. The cDNA samples were stored at -20 $^{\circ}$ C until further use.

qRT-PCR conditions: Amplification and detection of DNA by real-time PCR were performed with the ABI-PRISM 7700 Sequence Detection System (Applied Biosystems) using optical grade 96-well plates. Negative control of $\Delta sodB$ and RNase DNase free PCR water were used for amplification of *sodB* transcript and water was used as control in order to ensure the reactions were devoid of any cDNA contamination. The PCR reaction was performed in a total volume of 10 μ l using: 2 μ l of cDNA sample corresponding to 20 ng RNA, 5 μ l of TaqMan[®] Fast Universal PCR Master Mix 2x, 0.5 μ l TaqMan[®] probe, 0.5 μ l of 10 μ M forward primer, 0.5 μ l of 10 μ M reverse primer, 1.5 μ l of RNAase-DNase free PCR water. Sequences of probes and primers used for qPCR are listed in Table S2. The reactions were incubated in a plate at 95 $^{\circ}$ C for 20s, followed by 40 cycles of 95 $^{\circ}$ C for 1s and 60 $^{\circ}$ C for 20s. All reactions were run in duplicate samples. Data analysis made use of Sequence Detection Software version supplied by Applied Biosystems. The relative level of *sodB* transcript was calculated using a comparative Ct method (the threshold cycle (CT) is defined as the fractional cycle number at which the fluorescence passes the fixed

threshold.) and the housekeeping *rpsL* gene which encodes the 30S ribosomal protein S12 was used as an endogenous control.

Supplemental References

1. Arbel-Goren R, et al. (2013) Effects of post-transcriptional regulation on phenotypic noise in *Escherichia coli*. *Nucleic Acids Res* 41(9):4825–4834.
2. Baba T, et al. (2006) Construction of *Escherichia coli* K-12 in-frame, single-gene knockout mutants: the Keio collection. *Mol Syst Biol* 2:8.
3. Blattner FR, et al. (1997) The complete genome sequence of *Escherichia coli* K-12. *Science (80-)* 277(5331):1453–1462.
4. Masse E, Gottesman S (2002) A small RNA regulates the expression of genes involved in iron metabolism in *Escherichia coli*. *Proc Natl Acad Sci USA* 99(7):4620–4625.
5. Morita T, Maki K, Aiba H (2005) RNase E-based ribonucleoprotein complexes: mechanical basis of mRNA destabilization mediated by bacterial noncoding RNAs. *Genes Dev* 19(18):2176–86.
6. Siegele DA, Hu JC (1997) Gene expression from plasmids containing the araBAD promoter at subsaturating inducer concentrations represents mixed populations. *Proc Natl Acad Sci USA* 94(15):8168–8172.
7. Morgan-Kiss RM, Wadler C, Cronan Jr. JE (2002) Long-term and homogeneous regulation of the *Escherichia coli* araBAD promoter by use of a lactose transporter of relaxed specificity. *Proc Natl Acad Sci USA* 99(11):7373–7377.
8. Li XT, Thomason LC, Sawitzke JA, Costantino N, Court DL (2013) Positive and negative selection using the tetA-sacB cassette: recombineering and P1 transduction in *Escherichia coli*. *Nucleic Acids Res* 41(22):e204.
9. Datta S, Costantino N, Court DL (2006) A set of recombineering plasmids for gram-negative bacteria. *Gene* 379:109–115.
10. Dasgupta S, et al. (1998) Genetic uncoupling of the dsRNA-binding and RNA cleavage activities of the *Escherichia coli* endoribonuclease RNase III--the effect of dsRNA binding on gene expression. *Mol Microbiol* 28(3):629–40.
11. Sawitzke JA, et al. (2007) Recombineering: in vivo genetic engineering in *E. coli*, *S. enterica*, and beyond. *Methods Enzym* 421:171–199.
12. Thomason LC, Oppenheim AB, Court DL (2009) Modifying bacteriophage lambda with recombineering. *Methods Mol Biol* 501:239–251.
13. Yu D, et al. (2000) An efficient recombination system for chromosome engineering in *Escherichia coli*. *Proc Natl Acad Sci USA* 97(11):5978–5983.
14. Thomason LC, Costantino N, Court DL (2007) *E. coli* genome manipulation by P1 transduction. *Curr Protoc Mol Biol* Chapter 1:Unit 1 17.
15. So LH, et al. (2011) General properties of transcriptional time series in *Escherichia coli*. *Nat Genet* 43(6):554–560.

16. Crocker JC, Grier DG (1996) Methods of Digital Video Microscopy for Colloidal Studies. *J Colloid Interface Sci* 179(1):298–310.